Title	**Low-power wind energy conversion system with variable structure control for DC grids**
Author(s)	**Yang, Y; Mok, KT; Tan, SC; Hui, RSY**
Citation	**The 2014 IEEE 5th International Symposium on Power Electronics for Distributed Generation Systems (PEDG 2014), Galway, Ireland, 24-27 June 2014. In Conference Proceedings, 2014, p. 1-6**
Issued Date	**2013**
URL	**http://hdl.handle.net/10722/204067**
Rights	**Creative Commons: Attribution 3.0 Hong Kong License**

Low-Power Wind Energy Conversion System with Variable Structure Control for DC Grids

Yun Yang[1] *Student Member, IEEE*
Kwan-Tat Mok[1] *Student Member, IEEE*
Siew-Chong Tan[1] *Senior Member, IEEE*
S. Y. R. Hui[1,2] *Fellow, IEEE*

[1]Department of Electrical & Electronics Engineering
The University of Hong Kong
Hong Kong, China
Email:yangyun@eee.hku.hk

[2]Department of Electrical & Electronic Engineering
Imperial College London
London, United Kingdom
Email: r.hui@imperial.ac.uk

***Abstract*—This paper presents a discussion on the use of variable structure control, i.e., sliding mode control, for improving the dynamic control performance of a low-power wind energy conversion system (WECS) that is connected to a DC microgrid. The sliding mode control is applied to the wind turbine system to extract the maximum possible power from the wind, thus achieving the state of maximum power point tracking to reach the maximum power generation (MPG), and also applied to the power converter to reach the maximum power injection (MPI) to the load. The amount of energy extractable from a dynamically changing wind using the WECS with sliding mode control is compared with that of the classic PI controller. Simulation results show that for a dynamically changing wind, more energy can be harvested with the sliding mode control as compared to the PI control.**

***Index Terms*—Wind energy conversion system (WECS), variable structure control (VSC), maximum power generation (MPG), maximum power injection (MPI), maximum power flow.**

I. Introduction

For low-power wind energy conversion systems (WECS), the injected power is small relative to the power capacity of the entire system. All the energy harvested from the wind may be directly injected into the grid without the need for a local energy storage [1]–[3]. This is widely applied in microgrid systems [4]–[6]. Many research works on low-power WECS are focused on optimizing the energy conversion, interfacing wind turbines to the grid, and the reduction of the fatigue load of the mechanical structure [7]–[15]. In particular, maximum power point tracking (MPPT) control plays a crucial role in optimizing the efficiency of the energy conversion [16]–[20]. MPPT control is applicable not only to wind power system, but also to photovoltaic and water pumping systems. It covers an entire class of extremum search algorithms including hill-climbing search [21]–[23], tip-speed ratio control [24]–[26], perturbed and observed [27]–[29], power signal feedback control [6] etc. Literature review shows that applications of MPPT control in WECS is typically focused on the wind turbine part which is only concerned with the maximum power generation (MPG) capability, that is, to extract the maximum possible power from the wind. There is a lack of research on the MPPT control of the entire system, covering wind turbine generation, power electronics conversion, and microgrid current injection.

In WECS without energy storage, MPPT control of the system is achievable only if the MPG of wind turbine matches the maximum power injection (MPI) of the load, i.e., a maximum power flow taking place within the system. Moreover, conventional research are focused on the steady-state tracking of the MPPT. In reality, wind is a time-varying uncertain parameter, of which to achieve real-time MPPT control of the system, both the MPG and MPI must be matched dynamically via the control. Maximum power flow of the system and thus the state of MPPT, is non-achievable, otherwise. In that situation, part of the maximum power that could be extracted from the wind will be lost.

This paper discusses the use of variable structure control in the form of sliding mode (SM) control in a low-power WECS, to rapidly reach both MPG and MPI in the case of a dynamically changing wind such that MPPT of the system can be quickly attained to maximize the harvested energy. SM control is a robust control strategy that guarantees stability against parameter uncertainties, and it gives fast and consistent transient response performance in nonlinear systems that are operated with widely varying input and output conditions. The WECS system is highly nonlinear. With intermittent and dynamically varying wind power, the SM control will be more appropriate for the WECS system as compared to a typical proportional-integral (PI) controller. In this paper, the SM control is used for controlling both the wind turbine system and the voltage conversion system to respectively reach MPG and MPI such that maximum power is extracted from the wind and injected into the DC grid system. The energy extractable from wind and the transient performance of the system with the SM controller are compared to that of the PI controller.

II. Oerview of the System and Analysis of Wind Turbine Characteristics

An overview of the proposed DC grid-tied low-power WECS system and its control strategy is presented in Fig. 1. It comprises two subsystems, namely the wind turbine system and the voltage conversion system. The wind turbine

978-1-4799-5115-4/14/$31.00

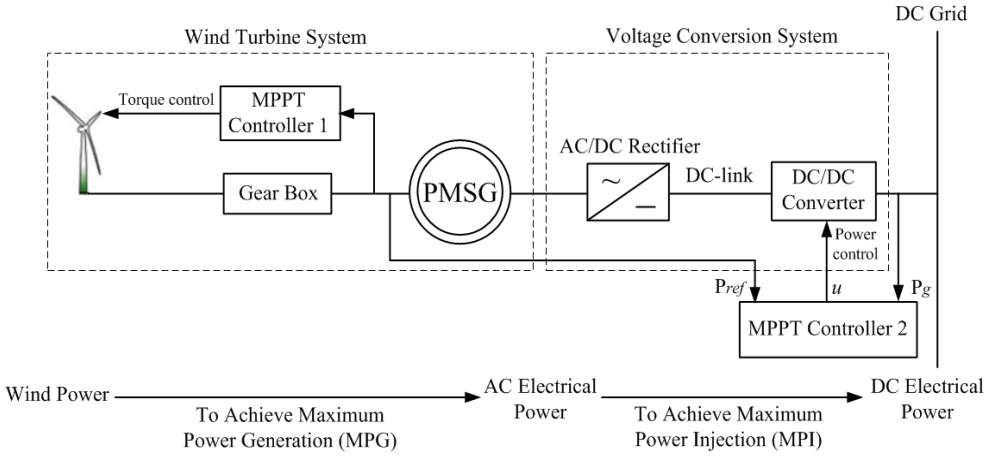

Fig. 1. Overview of a low-power WECS system.

system converts the wind energy into AC electrical energy. The function of the voltage conversion system is to convert the AC electrical voltage to the DC grid voltage level and to inject power to the grid. By applying MPPT scheme to control the torque of the wind turbine, MPG can be achieved. However, it must be emphasized that without a local storage, all power generated must be injected into the grid. If this is not achieved, the power generation will follow the grid-injected power and MPG will not be attained even if MPPT control is applied to the wind turbine system. The state of the voltage conversion system ensuring that the power generated from the wind turbine system with MPG are injected into the grid via the voltage conversion system will henceforth be known as MPI. To achieve MPI, the MPPT control must also be applied to the voltage conversion system such that its output power is specifically controlled such that the power generated from the wind turbine system through MPG matches the power injected into the grid.

In this system, the mechanical output power generated by the wind turbine is [6]

$$P_{out} = \frac{1}{2}\rho S_w v^3 C_p(\beta, \lambda), \tag{1}$$

where ρ is the air density; S_w is the swept area of the wind blade; v is the wind speed; $C_p(\beta, \lambda)$ is the conversion efficiency; β is the pitch angle of the blade; λ is the tip-speed ratio, where $\lambda = \frac{R\omega}{v}$; R is the blade radius; and ω is the angular velocity of the rotating blades. Here, the wind power level is low at only a few kilowatts. Therefore, a constant value of β is adopted [3]. According to [30], $C_p(\beta, \lambda)$ can be expressed as

$$C_p(\lambda) = 0.5176\left(\frac{116}{\lambda_i} - 5\right)e^{\frac{-21}{\lambda_i}} + 0.0068\lambda, \tag{2}$$

where $\frac{1}{\lambda_i} = \frac{1}{\lambda} - 0.035$. Then, the mechanical equation of the shaft can be expressed as [31]:

$$J\frac{d\Omega}{dt} = T_g - T_e - f\Omega, \tag{3}$$

where J and f are respectively the total moment of the inertia and the viscous friction coefficient; T_g is the gearbox torque; T_e is the generator torque; and Ω is the mechanical generator speed. By considering the gearbox, the following equation can be obtained

$$G = \frac{\Omega}{\Omega_t}, \tag{4}$$

where G is the gear ratio and Ω_t is the rotor speed of the turbine.

As the wind speed varies, the optimal value of λ must be maintained to ensure that the value of $C_p(\lambda)$ is at its maximum C_{pmax}. Since $\lambda = \frac{R\omega}{v}$, $\frac{\Omega_t}{v}$ should be constant. Thus, Ω_t is chosen to trace the variation of the wind speed. The wind power coefficient curve with a constant pitch can be plotted as shown in Fig. 2.

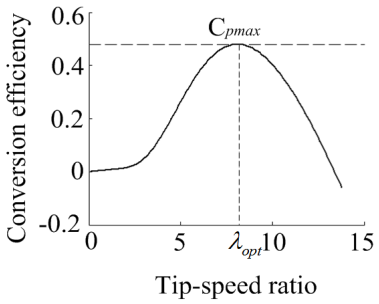

Fig. 2. Wind power coefficient curve for the wind turbine with a constant pitch.

III. SM Control Design for the System

The SM control is adopted in this work to control both the wind turbine system and the voltage conversion system. The control design is performed individually on the respective systems before they are being merged into a single system. The system performance will be compared with that of conventional PI controllers that are designed using the same approach.

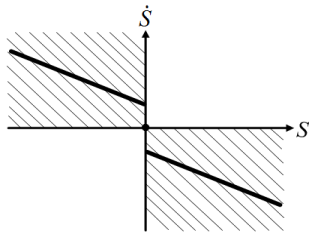

Fig. 3. SM dynamics for sliding surface.

A. SM Control Design of Wind Turbine System

According to (4) and the expression of the tip-speed ratio, the reference of the mechanical generator speed can be derived as

$$\Omega_{ref} = \frac{\lambda_{opt} v G}{R}. \tag{5}$$

The goal is to control the mechanical generator speed to run at this reference such that the tip-speed ratio is optimum, thereby leading to the generation of the maximum electrical output power. According to [32], the sliding surface is chosen as

$$S = \dot{\Omega}_{ref} - \dot{\Omega} + c \cdot (\Omega_{ref} - \Omega), \tag{6}$$

where c is a tuning factor. From (3), (5) and (6), we have

$$\begin{aligned} \dot{S} = &\left(\frac{f^2}{J^2} + \frac{c \cdot f}{J}\right) S + \left(\frac{f}{J^2} + \frac{c}{J}\right)(T_e - T_g) \\ &+ \ddot{\Omega}_{ref} + c \cdot \dot{\Omega}_{ref} - \left(\frac{f^2}{J^2} + \frac{c \cdot f}{J}\right) \Omega_{ref}. \end{aligned} \tag{7}$$

In order to satisfy the Lyapunov stability criteria $S \cdot \frac{dS}{dt} < 0$, (7) must be located in the shaded zones given in Fig. 3. A piecewise function form of (7) can meet such a requirement. The expression of the generator torque can be obtained as

$$\begin{aligned} T_e = T_g - f\Omega_{ref} + \alpha_1 \ddot{\Omega}_{ref} + \left(J - \frac{f}{J}\alpha_1\right) \dot{\Omega}_{ref} \\ + \alpha_2 \text{sign}(\Omega_{ref} - \Omega), \end{aligned} \tag{8}$$

where $\text{sign}(.)$ is the signum function. $\alpha_1 = \frac{J^2}{c \cdot J + f}$ and α_2 is a tuning factor.

B. SM Control Design of Voltage Conversion System

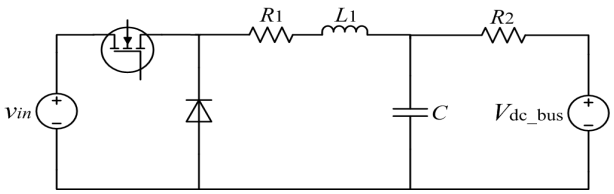

Fig. 4. Grid-tied DC/DC converter topology.

Fig. 4 shows the topology of the grid-tied DC/DC converter used in this system. With a widely-varying input voltage and input power, it can be equivalently considered as a general buck converter with widely-varying input voltage and load, which can be well regulated by SM controller [33]. The mathematical expression of the grid-tied DC/DC converter with SM controller is

$$\begin{cases} v_{in} \cdot u = L_1 \frac{di_{L_1}}{dt} + R_1 i_{L_1} + v_c \\ V_{dc} = -R_2 i_{L1} + R_2 C \frac{dv_c}{dt} + v_c \end{cases}. \tag{9}$$

The sliding surface selected is

$$S(\mathbf{x}, t) = \sum_{i=1}^{3} \alpha_i x_i(t), \tag{10}$$

where α_i represents sliding coefficients and $x_i(t) \in \mathbf{x}(t)$. Control variables chosen are

$$\mathbf{x} = \begin{bmatrix} x_1 \\ x_2 \\ x_3 \end{bmatrix} = \begin{bmatrix} v_{ref} - \beta v_c \\ \frac{d(v_{ref} - \beta v_c)}{dt} \\ \int (v_{ref} - \beta v_c) dt \end{bmatrix}. \tag{11}$$

The SM control strategy can be determined as

$$v_{con} = K_1 i_C + K_2 v_c + K_3 \tag{12}$$

and

$$v_{ramp} = \beta v_{in}, \tag{13}$$

where $K_1 = -\frac{\alpha_1 \beta L_1}{\alpha_2} + \beta\left(\frac{L_1}{R_2 C} + R_1\right)$, $K_2 = -\frac{\alpha_3 \beta L_1 C}{\alpha_2} + \beta\left(\frac{R_1}{R_2} + 1\right)$ and $K_3 = -\frac{\beta R_1}{R_2} V_{dc} + \frac{\alpha_3}{\alpha_2} L_1 C \left(\frac{P_{in} C_p(\lambda) \eta}{V_{dc}} R_2 + V_{dc}\right)$. The coefficients are selected to satisfy the hitting, existence, and stability conditions of sliding mode operation [33].

IV. Simulation Results

TABLE I
SPECIFICATIONS OF THE WIND TURBINE SYSTEM

Parameters	Values
Radius of Rotor	3 m
Number of blades	3
Density of air	1.225 kg/m^3
Gear ratio	5
Friction coefficient	0.002 $\text{N} \cdot \text{m/s}$
Turbine inertia	0.2 $\text{kg} \cdot \text{m}^2$

TABLE II
SPECIFICATIONS OF THE VOLTAGE CONVERTER SYSTEM

Parameters	Values	Parameters	Values
L_1	1.3 mH	R_1	0.2 Ω
R_2	0.2 Ω	C	20 μF
V_{dc_bus}	100 V	I_{out}	5.28 $\sim$ 42.21 A
v_{in}	200 $\sim$ 700 V	I_{in_max}	10 A

The specifications of the wind turbine system and the voltage conversion system used in the simulation are given in Table I and Table II, respectively. Generally, for a low-power wind system, the maximum wind speed is $v_{wind} = 12$ m/s and minimum wind speed is $v_{wind} = 6$ m/s [6]. A full power range of the wind speed changing from 6 m/s to 12 m/s is

applied for the optimal tuning of both the PI controller and the SM controller to achieve the best possible performance for this step change.

A. PI Control Versus SM Control of Wind Turbine System for Achieving MPG

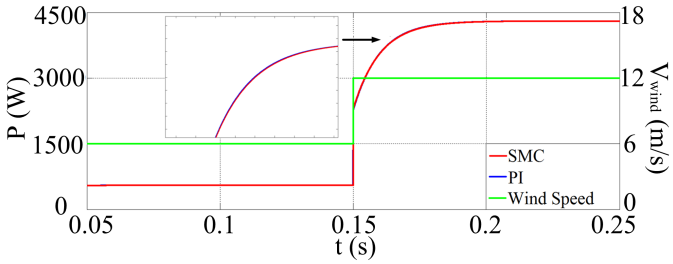

Fig. 5. Comparison of turbine-generated output power using PI control and SM control for full range condition.

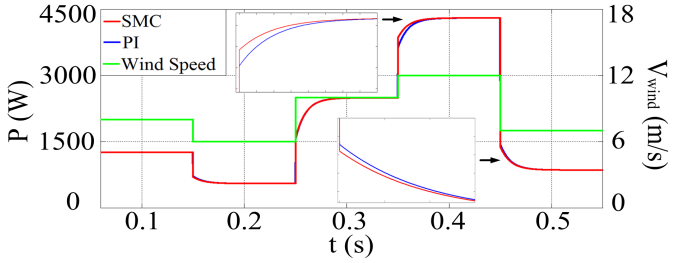

Fig. 6. Comparison of turbine-generated output power using PI control and SM control for various conditions of wind-speed step change.

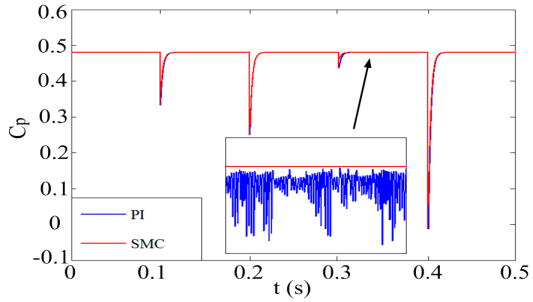

Fig. 7. Power conversion coefficient with PI control and SM control.

For the wind turbine system, the values of $K_p = 21.524$ and $K_i = 0.178$ are adopted in the PI control, where K_p is the proportional coefficient and K_i is the integral coefficient, and the value of $\alpha_1 = 0.01$ and $\alpha_2 = 100$ are chosen as the coefficients of the SM controller. Both these controllers are designed to give the same optimal performance in power extraction for a step change from $v_{wind} = 6$ m/s to $v_{wind} = 12$ m/s, and the simulated results are given in Fig. 5. However, with a change in the dynamic operating condition of the wind speed from its original condition, the results are different. The SM controller performs better in generating more power during the transient period in all situations than the PI controller,

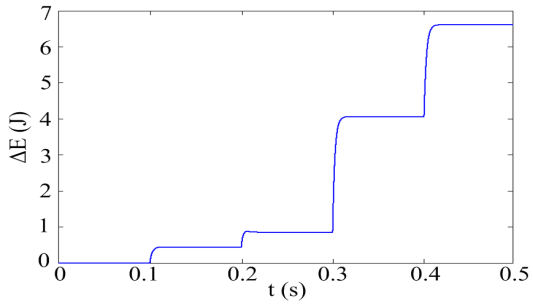

Fig. 8. Difference of energy acquired from the wind between the SM control (E_{SM}) and PI (E_{PI}) control, where $\Delta E(\mathrm{J}) = \mathrm{E_{SM}} - \mathrm{E_{PI}}$.

as shown in Fig. 6. This demonstrates the strength of SM control in handling dynamically varying operating conditions in nonlinear systems, which in this case, is to respond quickly to tracking the MPPT point for maximum power generation when wind speed varies. With the SM control always reaching the desired maximum power conversion coefficient faster than the PI control when wind speed changes (see in Fig. 7), the energy acquisition with the SM controller (i.e. E_{SM}) is larger than that with the PI controller (i.e. E_{PI}), as shown in Fig. 8.

B. PI Control Versus SM Control of the Voltage Conversion System for Achieving MPI

The same procedure is adopted for the design of the voltage conversion system. Full power range of the output current changing from 5.28 A to 42.21 A is applied for the optimal tuning of both the PI and SM controller. Here, for PI control, $K_p = 0.5$ and $K_i = 120$, and for SM control, $K_1 = 0.0153$, $K_2 = 7.2$, and $\beta = 0.025$. As shown in Fig. 9, both controllers have a similar transient performance. Then, a step change of the injected current of the grid-tied DC/DC converter from 12.51 A to 5.28 A to 24.43 A to 42.21 A to 8.38 A is performed to compare the performance of the two controllers, which is given in Fig. 10. For all these conditions, faster transient performance with less overshoot is achievable with the SM control.

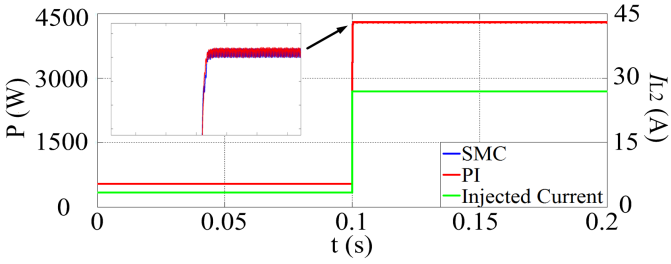

Fig. 9. Output power response of buck converter with PI control and SM control for full injected current range.

C. Overall System Controlled by PI Controller and SM Controller

With the PI controllers and SM controllers optimally tuned for the respective wind turbine and voltage conversion system,

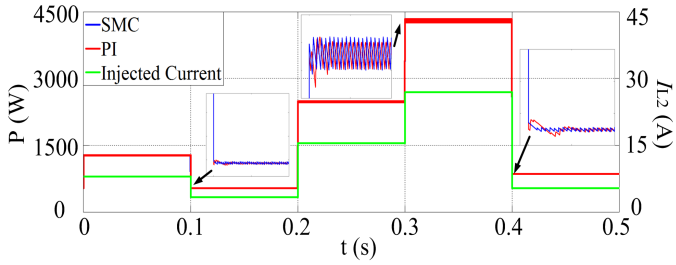

Fig. 10. Output power response of buck converter with PI control and SM control for varying injected current step changes.

both these systems are then connected together for operation. It is found that the optimally tuned system with PI control is no longer optimal when operated as a whole system for wind speed changing from 6 m/s to 12 m/s as compared to the system with SM control, which still performs optimally, as illustrated in Fig. 11. Also, wind speed changing from 8 m/s to 6 m/s to 10 m/s to 12 m/s to 7 m/s at every 0.1 s are applied. The waveforms provided in Fig. 12 show that the so-called optimally-tuned PI controllers are incapable of tracking the desired parameters of such a non-linearly cascaded system with widely varied operating conditions. Its transient performance is poor as compared to that achievable with SM control, which gives a robust performance for all changes. With a wind speed that changes repeatedly from 8 m/s to 6 m/s to 10 m/s to 12 m/s to 7 m/s over a period of five minutes, the energy acquisition for the overall system by both SM and PI controllers and the difference in their energy acquisition are simulated and are respectively shown in Figs. 13 and 14. The results show that more energy can be harvested from the system with the SM controller.

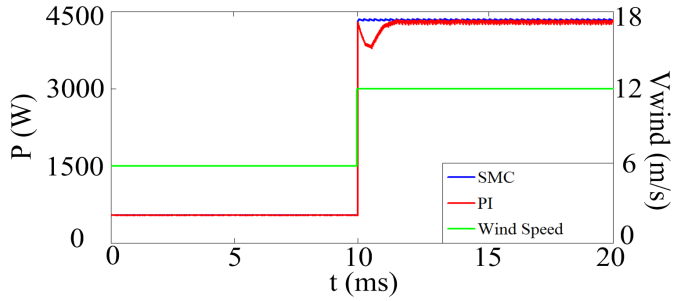

Fig. 11. Overall system performances for PI control and SM control for full range operating condition.

V. Conclusions

In this paper, a low-power wind energy conversion system with variable structure control is proposed for DC grids. To illustrate the capability of this non-linear controller, a comparison of the system in harvesting wind power with the linear PI controller is performed. Results show that the SM controller has a better transient tracking ability than a PI controller in terms of extracting power in a varying wind speed operating condition. The SM controller also show its

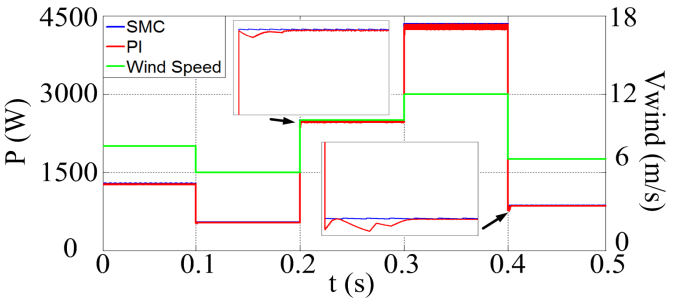

Fig. 12. Overall system performances of the PI control and the SM control for varying wind-speed step change conditions.

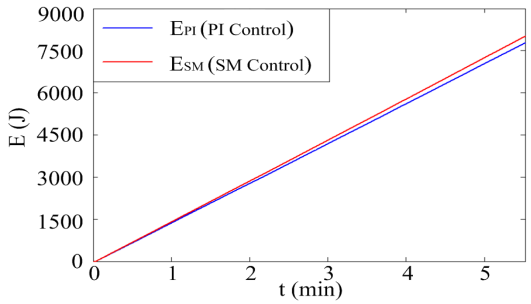

Fig. 13. Energy acquisition by SM controller and PI controller for the overall system.

robustness in maximizing power transfer from wind energy to the micro-grid current injection. Overall, the SM controller allows more power to be extracted from the wind in the dynamical scenario than the PI controller.

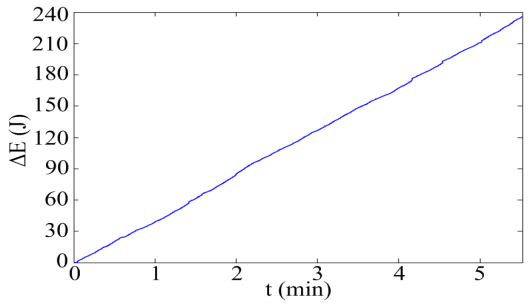

Fig. 14. Difference of energy acquired from the wind between the SM control (E_{SM}) and PI (E_{PI}) control, where $\Delta E(\mathrm{J}) = \mathrm{E_{SM}} - \mathrm{E_{PI}}$.

References

[1] S. M. Muyeen, R. Takahashi, T. Murata, and J. Tamura, "Integration of an energy capacitor system with a variable-speed wind generator," *IEEE Trans. Energy Convers.*, vol. 24, no. 3, pp. 740–749, Sept. 2009.

[2] M. Black and G. Strbac, "Value of bulk energy storage for managing wind power fluctuations," *IEEE Trans. Energy Convers.*, vol. 22, no. 1, pp. 197–205, Mar. 2007.

[3] D. D. Banham-Hall, G. A. Taylor, C. A. Smith, and M. R. Irving, "Flow batteries for enhancing wind power integration," *IEEE Trans. Power Syst.*, vol. 27, no. 3, pp. 1690–1697, Aug. 2012.

[4] J. Wang, D. Xu, B. Wu, and Z. Luo, "A low-cost rectifier topology for variable-speed high-power PMSG wind turbines," *IEEE Trans. Power Electron.*, vol. 26, no. 8, pp. 2192–2200, Aug. 2011.

[5] S. Alepuz, A. Calle, S. Busquets-Monge, S. Kouro, and B. Wu, "Use of stored energy in PMSG rotor inertia for low-voltage ride-through in back-to-back NPC converter-based wind power systems," *IEEE Trans. Ind. Electron.*, vol. 60, no. 5, pp. 1787–1796, May 2013.

[6] I. Munteanu, N. A. Cutululis, A. I. Bratcu, and E. Ceanga, *Optimal Control of Wind Energy Systems : Towards a Global Approach*, Springer, 2008.

[7] Y. Wang, D. Panda, T. A. Lipo, and P. Di, "Open-winding power conversion systems fed by half-controlled converters," *IEEE Trans. Power Electron.*, vol. 28, no. 5, pp. 2427–2436, May 2013.

[8] D. Battista, P. F. Puleston, R. J. Mantz, and C. F. Christiansen, "Sliding mode control of wind energy systems with DOIG-power efficiency and torsional dynamics optimization," *IEEE Power Syst.*, vol. 15, no. 2, pp. 728–734, May 2000.

[9] B. G. Rawn, P. W. Lehn, and M. Maggiore, "Control methodology to mitigate the grid impact of wind turbines," *IEEE Trans. Energy Convers.*, vol. 22, no. 2, pp. 431–438, June 2007.

[10] K. Y. Lo, Y. M. Chen, and Y. R. Chang, "MPPT battery charger for stand-alone wind power system," *IEEE Trans. Power Electron.*, vol. 26, no. 6, pp. 1631–1638, June 2011.

[11] P. Wang, Z. Gao, and L. Bertling, "Operational adequacy studies of power systems with wind farms and energy storages," *IEEE Power Syst.*, vol. 27, no. 4, pp. 2377–2384, Nov. 2012.

[12] Y. K. Tan and S. K. Panda, "Optimized wind energy harvesting system using resistance emulator and active rectifier for wireless sensor nodes," *IEEE Trans. Power Electron.*, vol. 26, no. 1, pp. 38–50, Jan. 2011.

[13] Y. Tang and L. Xu, "A flexible active and reactive power control strategy for a variable speed constant frequency generating system," *IEEE Trans. Power Electron.*, vol. 10, no. 4, pp. 472–478, July 1995.

[14] Y. Juan, "An integrated-controlled AC/DC interface for microscale wind power generation systems," *IEEE Trans. Power Electron.*, vol. 26, no. 5, pp. 1377–1384, May 2011.

[15] V. Kumar, R. R. Joshi, and R. C. Bansal, "Optimal control of matrix-converter-based WECS for performance enhancement and efficiency optimization," *IEEE Power Syst.*, vol. 27, no. 4, pp. 2377–2384, Nov. 2012.

[16] Y. Xia, K. H. Ahmed, and B. W. Williams, "A new maximum power point tracking technique for permanent magnet synchronous generator based wind energy conversion system," *IEEE Trans. Power Electron.*, vol. 26, no. 12, pp. 3609–3620, Dec. 2011.

[17] S. M. R. Kazmi, H. Goto, H. J. Guo, and O. Ichinokura, "A novel algorithm for fast and efficient speed-sensorless maximum power point tracking in wind energy conversion system," *IEEE Trans. Ind. Electron.*, vol. 58, no. 1, pp. 29–36, Jan. 2011.

[18] C. T. Pan and Y. L. Juan, "A novel sensorless MPPT controller for a high-efficiency microscale wind power generation system," *IEEE Trans. Energy Convers.*, vol. 25, no. 1, pp. 207–216, Mar. 2010.

[19] R. M. Hilloowala and A. M. Sharaf, "A utility interactive wind energy conversion scheme with an asynchronous DC link using a supplementary control loop," *IEEE Trans. Energy Convers.*, vol. 9, no. 3, pp. 558–563, Sept. 1994.

[20] I. Tsoumas, A. Safacas, E. Tsimplostefanakis, and E. Tatakis, "An optimal control strategy of a variable speed wind energy conversion system," *IEEE Trans. Energy Convers.*, vol. 9, no. 3, pp. 558–563, Sept. 1994.

[21] R. Datta and V. T. Ranganathan, "A method of tracking the peak power points for a variable speed wind energy conversion system," *IEEE Trans. Energy Convers.*, vol. 18, no. 1, pp. 163–168, Mar. 2003.

[22] K. Tan and S. Islam, "Optimum control strategies in energy conversion of PMSG wind turbine system without mechanical sensors," *IEEE Trans. Energy Convers.*, vol. 19, no. 2, pp. 392–399, June 2004.

[23] Q. Wang and L. Chang, "An intelligent maximum power extraction algorithm for inverter-based variable speed wind turbine systems," *IEEE Trans. Power Electron.*, vol. 19, no. 5, pp. 1242–1249, Sept. 2004.

[24] B. Beltran, T. Ahmed-Ali, and M. E. H. Benbouzid, "Sliding mode power control of variable-speed wind energy conversion systems," *IEEE Trans. Energy Convers.*, vol. 23, no. 2, pp. 551–558, June 2008.

[25] H. De Battista, R. J. Mantz, and C. F. Christiansen, "Dynamical sliding mode power control of wind driven induction generators," *IEEE Trans. Energy Convers.*, vol. 15, no. 4, pp. 451–457, Dec. 2000.

[26] B. Beltran, T. Ahmed-Ali, and M. Benbouzid, "High-order sliding-mode control of variable-speed wind turbines," *IEEE Trans. Ind. Electron.*, vol. 56, no. 9, pp. 3314–3321, Sept. 2009.

[27] Y. Xia, K. H. Ahmed, and B. W. Williams, "Wind turbine power coefficient analysis of a new maximum power point tracking technique," *IEEE Trans. Ind. Electron.*, vol. 60, no. 3, pp. 1122–1132, Mar. 2013.

[28] Z. M. Dalala, Z. U. Zahid, and J. S. Lai, "New overall control strategy for small-scale WECS in MPPT and stall regions with mode transfer control," *IEEE Trans. Energy Convers.*, vol. 28, no. 4, pp. 1082–1092, Dec. 2013.

[29] Z. M. Dalala, Z. U. Zahid, W. Yu, and Y. Cho, "Design and analysis of an MPPT technique for small-scale wind energy conversion systems," *IEEE Trans. Energy Convers.*, vol. 28, no. 3, pp. 756–767, Sept. 2013.

[30] V. Akhmatov, "Variable-speed wind turbines with doubly-fed induction generators. Part IV: uninterrupted operation features at grid faults with converter control coordination," *Wind Eng.*, vol. 26, no. 2, pp. 519–529, July 2009.

[31] S. Heier, *Grid Integration of Wind Energy Conversion Systems*, John Wiley & Sons Ltd, 1998.

[32] V. I. Utkin, "Sliding mode control design. principles and applications to electric drives," *IEEE Trans. Ind. Electron.*, vol. 40, no. 1, pp. 23–36, Jan. 1993.

[33] S. C. Tan, Y. M. Lai, and C. K. Tse, *Sliding Mode Control of Switching Power Converters - Techniques and Implementation*, CRC, 2012.